All-Electrical Nuclear Spin Polarization of Donors in Silicon

C. C. Lo, C. D. Weis, J. van Tol, J. Bokor, and T. Schenkel

All-electrical nuclear spin polarization of donors in silicon

C. C. Lo[1,2],[*] C. D. Weis[1], J. van Tol[3], J. Bokor[2,4], and T. Schenkel[1]

[1]*Accelerator and Fusion Research Division, Lawrence Berkeley National Laboratory, Berkeley, California 94720, U.S.A.*
[2]*Department of Electrical Engineering and Computer Sciences,*
University of California, Berkeley, California 94720, U.S.A.
[3]*National High Magnetic Field Laboratory, Tallahassee, Florida and*
[4]*The Molecular Foundry, Lawrence Berkeley National Laboratory, Berkeley, California 94720, U.S.A.*

We demonstrate an all-electrical donor nuclear spin polarization method in silicon by exploiting the tunable interaction of donor bound electrons with a two dimensional electron gas (2DEG), and achieve over two orders of magnitude nuclear hyperpolarization at $T = 5$ K and $B = 12$ T with an in-plane magnetic field. We also show an intricate dependence of nuclear polarization effects on the orientation of the magnetic field, and both hyperpolarization and antipolarization can be controllably achieved in the quantum Hall regime. Our results demonstrate that donor nuclear spin qubits can be initialized through local gate control of electrical currents without the need for optical excitation, enabling the implementation of nuclear spin qubit initialization in dense multi-qubit arrays.

One of the requirements for constructing a scalable quantum computer architecture is the ability to initialize the qubit [1]. While donor nuclear spin qubits [2] are well protected from decoherence sources and hence have extraordinarily long coherence times [3–5], they are also difficult to initialize. Several nuclear polarization schemes, such as those based on dynamic nuclear polarization (DNP) with electron spin resonance [6–14] or optical excitations [15–18] have been demonstrated so far. However, for the implementation in a scalable quantum computer architecture, it is crucial that the selected nuclear spin qubits can be addressed and initialized locally, which is difficult using optical excitation, hence an all-electrical initialization scheme is desired. Recently, a fast all-electrical nuclear spin initialization scheme for donor nuclear spins integrated in silicon nano-transistors was proposed by Stemeroff and de Sousa [19], but is yet to be experimentally demonstrated. Another all-electrical approach is to utilize nearby conduction electrons to initialize the nuclear spin [20, 21]. Here, we demonstrate this all-electrical nuclear spin polarization scheme with phosphorus (^{31}P) donors in silicon field-effect transistors (FETs). We also investigate donor polarization in the integer quantum Hall regime, which is of considerable interest for realizing single spin readout [22], qubit coupling and quantum communication [23, 24]. Our results show that careful tuning of the 2DEG density-of-states and bias fields can be used to controllably achieve hyper- (positive) and anti- (negative) polarization of donor nuclear spins.

Fig. 1(a) shows the energy levels of the nuclear spin-1/2 ^{31}P donors in the high field limit. τ_d denotes the donor electron (d) spin relaxation time, and τ_X the donor nuclear (n) spin relaxation time due to an electron-nuclear flip-flop process [3]. As $\tau_X \propto 1/B^2 T_p A^2 I$ [8], where B is the magnetic field, T_p the surrounding phonon bath temperature, A the Fermi contact hyperfine constant, and I the nuclear spin, this process becomes efficient at high magnetic fields and we expect $\tau_X \approx 10$ s at 12 T and 5 K [15]. When donors interact with conduction electrons (c) such as those from a nearby two-dimensional electron gas (2DEG) (Fig. 1(b) and (c)) with orbital temperature T_c (the temperature which governs the distribution function of the 2DEG), the donor electron spin transitions are dominated by exchange interactions with conduction electrons [25]. These transition rates are denoted by Γ_{ex}^+ for the process involving a donor electron upwards transition (downwards for the conduction electron): $|\!\Downarrow_d\uparrow_c\rangle \rightarrow |\!\Uparrow_d\downarrow_c\rangle$, and Γ_{ex}^- for the opposite process involving a donor electron downwards transition: $|\!\Uparrow_d\downarrow_c\rangle \rightarrow |\!\Downarrow_d\uparrow_c\rangle$. While the conduction electrons can interact with the donor nuclei through direct hyperfine interaction, *i.e.* Korringa relaxation [26], this effect is small in semiconductors [19].

Under thermal equilibrium conditions, the donor electron spin temperature T_d^s and the phonon temperature T_p are equal and the relative populations of the four donor states are described by their respective Boltzmann factors. If T_d^s and T_p are different, *nuclear* polarization can result as the τ_d and τ_X processes will try to bring the populations back to their respective governing temperatures [20]. Fig. 1(d) shows the calculated nuclear polarizations achievable under different T_d^s and T_p at $B = 12$ T for ^{31}P donors. For donors embedded in FET devices, the donor electrons can interact with the gate-induced 2DEG [25, 27–31], and we use electrically detected magnetic resonance (EDMR) to quantify the resultant nuclear polarizations. While the resonant excitations during the readout phase of our experiments can potentially induce a conventional DNP process [9, 10, 32], in our experiments we can measure both nuclear hyperpolarization and antipolarization, and the polarizations obtained are robust against the direction of the magnetic field sweeps.

---

[*]Please contact the corresponding author under cheuk.lo@ucl.ac.uk.; Present address: London Centre for Nanotechnology, University College London, 17-19 Gordon Street, London WC1H 0AH, United Kingdom.
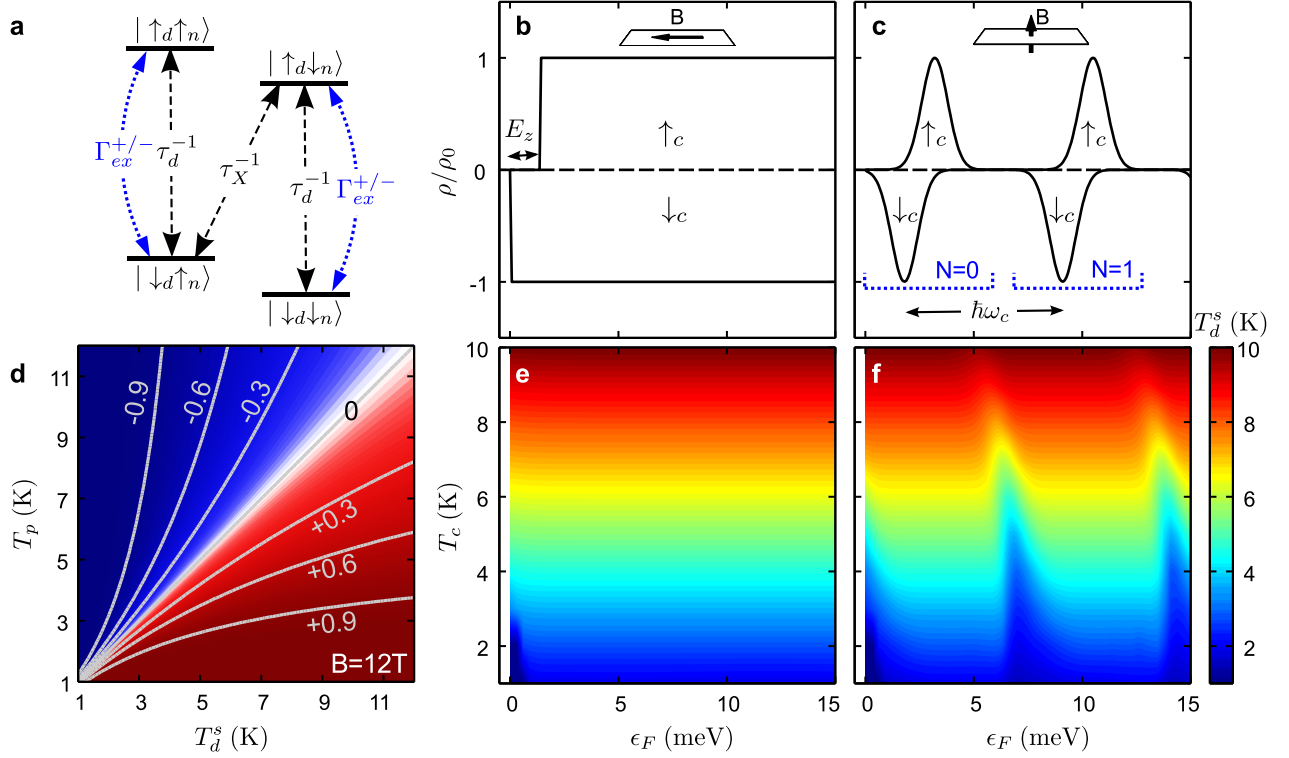
FIG. 1: (a) Energy levels of the Si:^{31}P system. Exchange interactions (blue) dominate the electron spin relaxation in the presence of conduction electrons. Schematics of the 2DEG density-of-states ρ under strong (b) in-plane ($\rho_0 = g_v(m^*/2\pi\hbar^2)$) and (c) out-of-plane ($\rho_0 = g_v(qB/h)/\sqrt{2\pi}\Gamma$) magnetic fields. (d) Calculated ^{31}P donor nuclear polarization resulting from a difference in T_p and T_d^s at $B = 12$ T. Calculated donor electron spin temperature T_d^s as T_c and ϵ_F are varied for (e) in-plane and (f) out-of-plane magnetic fields.
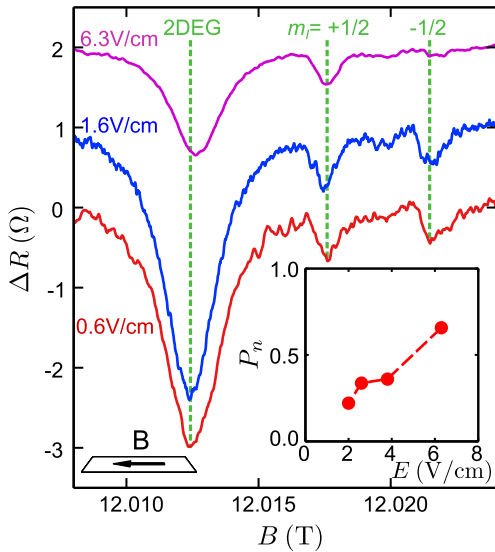

FIG. 2: EDMR spectra obtained with the in-plane magnetic field configuration and various bias E-fields at $T = 5$ K. Inset: ^{31}P nuclear polarization P_n measured under a constant current bias of $I_{DS} = 2000$ nA while the bias E-field is varied by adjusting the gate voltage V_g.

These imply the conventional DNP process is not playing a major role as the microwave power is relatively weak and the field sweeps are fast (> 0.1 mT/s), hence the resonant electron spin transitions are not sufficient to perturb the nuclear polarizations. Instead, the detected nuclear polarizations are due to "heating" or "cooling" of T_d^s with respect to T_p by the interacting 2DEG.

The experiments were carried out with a high magnetic field heterodyne electron spin resonance spectrometer with 336 GHz microwave excitation [33, 34], and we monitor the changes in the device resistance under constant current bias while sweeping the magnetic field around $B = 12$ T. The FETs were built on nominally undoped natural $\langle 100 \rangle$ silicon wafers with a 1 μm thick isotopically enriched 99.95% ^{28}Si layer with 3×10^{16}/cm^3 ^{31}P donors grown on top. We note that only donors close to the FET channel ($\leq 10 - 30$ nm from the Si-SiO$_2$ interface depending on the gate bias [25]) with strong interaction with the gate-induced conduction electrons are polarized and detected in our measurements. The devices used have gate lengths of 160 μm and widths of 10 μm for in-plane magnetic field and 20 μm for out-of-plane magnetic field measurements. The gate oxides have thicknesses of 20 nm and effective low-field mobilities of 1.2 m^2/Vs at $T = 5$ K.

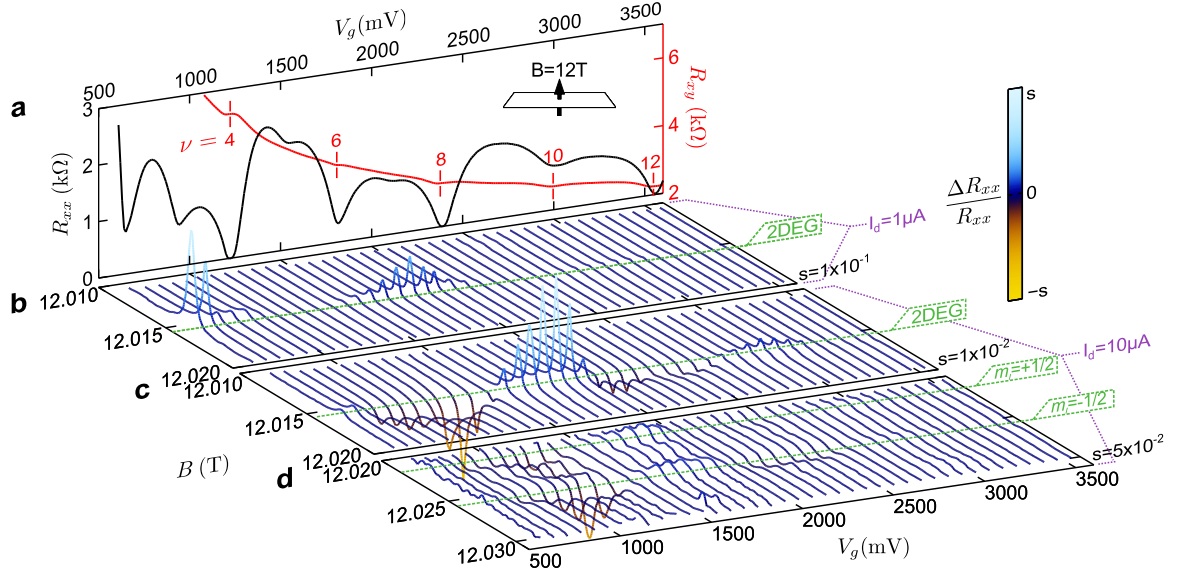The orientation of the applied magnetic field plays a

FIG. 3: (a) Longitudinal (R_{xx}, black) and transverse (R_{xy}, red) resistances measured with $I_{DS} = 2\,\mu A$ at $T = 3\,K$ under a fixed out-of-plane magnetic field of $B = 12\,T$, as illustrated in the inset. (b) EDMR measurements of ΔR_{xx} with a fixed bias current of $I_{DS} = 1\,\mu A$ at $T = 5\,K$ showing the 2DEG resonance signal. (c) - (d) EDMR measurements with $I_{DS} = 10\,\mu A$ under otherwise identical conditions, showing the 2DEG and donor resonance signals, respectively. The scale s of the EDMR signals are indicated to the right of each plot.

crucial role in the transport behavior of the 2DEG itself [35], and we will first discuss nuclear polarization with an in-plane magnetic field. Fig. 2 shows the change in the drain-source resistance ΔR across the spin resonance conditions. We will use the convention that $\Delta R = R_{res} - R$ throughout, where R_{res} and R are the on- and off-resonance resistance, respectively. Under a low bias electric field of $E = 0.6$ V/cm (current bias $I_{DS} = 200$ nA), the 2DEG and hyperfine-split ^{31}P donor signals are clearly observed, with the two donor signals having almost equal intensity. The high-field donor signal ($|\Downarrow_n\rangle, m_I = -1/2$) diminishes compared to the low-field line ($|\Uparrow_n\rangle, m_I = +1/2$) when the bias electric field is increased. At the high bias of $E = 6.3$ V/cm ($I_{DS} = 2000$ nA), we find a nuclear polarization of $P_n = (y_{\uparrow_n} - y_{\downarrow_n})/(y_{\uparrow_n} + y_{\downarrow_n}) = +0.66$, where $y_{\uparrow_n/\downarrow_n}$ are the amplitudes of Gaussian fits to the signals. This polarization corresponds to an 800-fold enhancement from thermal equilibrium and has an effective nuclear spin temperature of 6.3 mK. As we will show later, the donor electron spin temperature T_d^s is almost always equal to the 2DEG orbital temperature T_c with this in-plane field configuration, hence T_d^s increases with bias current as the 2DEG gets "hot" with increased electric fields. While the hot 2DEG will also increase the surrounding lattice temperature, the phonon temperature T_p seen by donors is lower due to the large heat capacity of the bulk silicon lattice. This situation with $T_d^s \approx T_c > T_p$ results in hyperpolarization of the nuclear spin. From Fig. 1(d), a temperature difference between T_d^s and T_p of approximately 5 K is needed to achieve the observed nuclear polarization at $T_p = 5$ K, which is consistent with the

electric field applied to the device [35]. The inset of Fig. 2 shows the gate-controlled nuclear polarization achievable under constant current bias.

We observe integer quantum Hall effects by applying the magnetic field out-of-plane of the 2DEG, and Fig. 3(a) shows the longitudinal resistance R_{xx} and transverse resistance R_{xy} of a device with Hall bar geometry at 12 T. At this field, the silicon 2DEG has a Landau level (LL) separation $\hbar\omega_c = 7.3$ meV much larger than the Zeeman splitting of $E_z = 1.4$ meV (Fig. 1(c)). In EDMR measurements under a relatively low current bias of $I_{DS} = 1\ \mu A$, a change in R_{xx} corresponding to the 2DEG resonance signal appears only when the Fermi level lies within the spin-slitting of a given LL, i.e. for filling factors of $\nu \approx 2, 6, 10, ... = 4N + 2$ as shown in Fig. 3(b), where $N = 0, 1, 2, ...$ is the LL index. This situation is analogous to the 2DEG spin resonance signals observed in GaAs [32, 36, 37]. We note that the values of ν for which the 2DEG spin resonances appears in GaAs and $\langle 100 \rangle$ Si differ due to the two-fold valley degeneracy in the latter [35].

Fig. 3(c) shows the EDMR spectra obtained under a higher bias current of $I_{DS} = 10\ \mu A$, where the 2DEG resonance signal shows an oscillatory behavior with positive and negative signs of ΔR_{xx}. Matsunami et al have previously shown oscillatory 2DEG resonance signals in high-mobility SiGe 2DEGs in the quantum Hall regime by controlling the relative amplitudes of the cyclotron and Zeeman splittings, and demonstrated that resonant heating and electron polarization reduction cause two distinct resonance signatures with opposite signs [38–40]. While we have the cyclotron and Zeeman splittings fixed in our

measurements, under high bias current we are thermally exciting carriers of the 2DEG, which allow us to observe the reduction in electron polarization even when ϵ_F is between adjacent LLs — around the resistivity minima of $\nu = 4(N+1)$. We also detect the donor resonance signals in the quantum Hall regime due to the polarization transfer mechanism [31] as shown in Fig. 3(d). The extracted donor nuclear spin polarizations as a function of bias current for the filling factors $\nu = 1$ ($V_g = 380$ mV, not shown in Fig. 3 since the low carrier density prevents the application of large bias currents) and $\nu = 4$ ($V_g = 1222$ mV) are shown in Fig. 4. In the first case, the hot electron mechanism as described for the in-plane magnetic field configuration dominates and hyperpolarization increases with higher current bias. In the latter case, antipolarization results and diminishes with increasing bias current.

We will now examine the donor nuclear hyper- and antipolarization observed by considering the exchange interaction occurring in the presence of the 2DEG. The donor electron spin relaxation time is dominated by the exchange interaction with the 2DEG in our system, hence $\tau_d^{-1} \approx \Gamma_{ex}^+ + \Gamma_{ex}^-$ [25]. The exchange scattering rates for the donor electron upward (+) and downward (−) spin transitions are given by:

$$\Gamma_{ex}^{+/-} = \frac{2\pi}{h}|J|^2 \int_0^\infty \left[\rho^{\uparrow_c/\downarrow_c}(\epsilon)f(\epsilon - \epsilon_F)\right] \times \\ \left[\rho^{\downarrow_c/\uparrow_c}(\epsilon \mp E_z)\left(1 - f(\epsilon \mp E_z - \epsilon_F)\right)\right] d\epsilon \quad (1)$$

where h is Plank's constant, J the exchange interaction strength determined by the wave function overlap of the 2DEG and donor electrons, $\rho^{\uparrow_c}(\epsilon)$ and $\rho^{\downarrow_c}(\epsilon)$ the 2DEG density-of-states at energy ϵ for spin up and down conduction electrons, respectively, ϵ_F the Fermi energy, and f the Fermi function at the 2DEG temperature T_c. Using Eq. 1 we can obtain the effective donor electron spin temperature T_d^s by calculating the
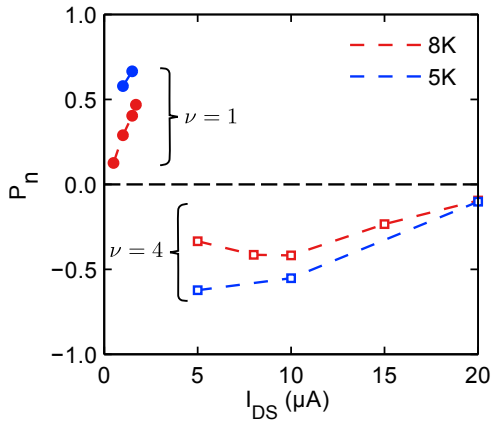

FIG. 4: Bias current dependence of the donor nuclear spin polarization P_n measured at $T = 5$ and 8 K for $\nu = 1$ (closed circles) and $\nu = 4$ (open squares). The dashed lines are guides for the eyes.

ratio of the upwards to downward transition rates as $N_{\uparrow_d}/N_{\downarrow_d} \approx \Gamma_{ex}^+/\Gamma_{ex}^- = \exp(-E_z/k_B T_d^s)$, where N_i is the electron population of state i. The magnitudes of $\Gamma_{ex}^{+/-}$ are sensitive to $\rho^{\uparrow_c/\downarrow_c}(\epsilon)$, and these are shown for the in-plane and out-of-plane magnetic field configurations in Figs. 1(b) and 1(c), respectively, where we have assumed an ideal 2DEG and $\rho^{\uparrow_c/\downarrow_c}(\epsilon)$ consists of Gaussians in the quantum Hall regime with a broadening parameter $\Gamma = 1$ meV. We also note that the LL and valley occupancies for a 2DEG electron does not change upon spin exchange interaction with a donor electron.

Figs. 1(e) and (f) shows the resulting effective donor spin temperatures T_d^s as a function of the 2DEG orbital temperature T_c. We note that when the 2DEG is highly polarized around the Fermi level, such as when $\epsilon_F \ll E_z$ (around $\epsilon_F = 0$ meV or at the onset of each LL in Fig. 1(f)), $\Gamma_{ex}^- \gg \Gamma_{ex}^+$: the polarized conduction electrons flip donor electron spins downward and an effective cooling of T_d^s occurs. However, as T_c increases this cooling effect diminishes as the thermal energy becomes large compared to E_z, and the asymmetry in the exchange transition rates reduces. In the quantum Hall regime, the hyperpolarization observed for $\nu = 1$ implies that the hot electron effect still dominates at this low carrier density range even though exchange cooling should already be occurring. On the other hand, as we approach $\nu = 4$, the virtual cooling effect dominates and hence antipolarization is observed. The effect of increasing T_c can be seen in Fig. 4 as well when the antipolarization reduces with increasing current density.

In conclusion, we have realized donor nuclear hyper- and anti- polarization for ^{31}P donors in silicon FETs with P_n ranging from +0.66 to −0.62 for $T = 5$ K and $B = 12$ T, corresponding to effective nuclear spin temperatures of 6.3 mK and −6.8 mK, respectively. This work demonstrates all-electrical donor nuclear polarization with microscopic silicon devices, which can be scaled to ≈ 10 nm dimensions, and utilizing alternative shallow dopants with larger hyperfine interactions and nuclear spins, such as ^{209}Bi [18, 41] can further enhance the efficiency of the process. This technique of utilizing gate-induced conduction electrons for nuclear spin initialization is fully compatible with devices for single donor spin readout [42, 43] and with scalable donor spin qubit architectures for silicon-based quantum information processing.

[1] D. P. DiVincenzo. *Fortschr. Phys.*, 48(9):771, 2000.

[2] B. Kane. *Nature*, 393:133, 1998.

[3] G. Feher and E. Gere. *Physical Review*, 114(5):1245, 1959.

[4] M. Steger *et al. Science*, 336:1280, 2012.

[5] A. M. Tyryshkin *et al. Nature Materials*, 11(2):143, 2012.

[6] G. Feher. *Physical Review*, 103:500, 1956.

[7] G. Feher and E. A. Gere. *Physical Review*, 103:501, 1956.

[8] D. Pines, J. Bardeen, and C. P. Slichter. *Physical Review*, 106(3):489, 1957.

[9] H. Hayashi, T. Itahashi, and K. M. Itoh. *Physical Review B*, 80:045201, 2009.

[10] A. E. Dementyev, D. G. Cory, and C. Ramanathan. *The Journal of Chemical Physics*, 134(15):154511, 2011.

[11] W. G. Clark and G. Feher. *Physical Review Letters*, 10(4):134, 1963.

[12] M. J. R. Hoch *et al. Physical Review B*, 72(23):233204, 2005.

[13] Y. Komori and T. Okamoto. *Applied Physics Letters*, 90(3):032102, 2007.

[14] C. R. Dean *et al. Physical Review B*, 80(15):153301, 2009.

[15] D. R. McCamey *et al. Physical Review Letters*, 102(2):027601, 2009.

[16] A. Yang *et al. Physical Review Letters*, 102(25):257401, 2009.

[17] D. R. McCamey *et al. Science*, 330:1652, 2010.

[18] G. W. Morley *et al. Nature Materials*, 9:725, 2010.

[19] N. Stemeroff and R. de Sousa. *Physical Review Letters*, 107(19):197602, 2011.

[20] G. Feher. *Physical Review Letters*, 3(3):135, 1959.

[21] S Das Sarma *et al. IEEE Transactions on Magnetics*, 36(5):2821, 2000.

[22] D. Sleiter *et al. New Journal of Physics*, 12:093028, 2010.

[23] D. Mozyrsky, V. Privman, and M. L . Glasser. *Physical Review Letters*, 86(22):5112, 2001.

[24] T. Machida *et al. Applied Physics Letters*, 82(3):409, 2003.

[25] R. de Sousa, C. C. Lo, and J. Bokor. *Physical Review B*, 80:045320, 2009.

[26] A. Berg *et al. Physical Review Letters*, 64(21):2563, 1990.

[27] R. N. Ghosh and R.H. Silsbee. *Physical Review B*, 46(19):12508, 1992.

[28] C. C. Lo *et al. Applied Physics Letters*, 91(24):242106, 2007.

[29] L. H. Willems van Beveren *et al. Applied Physics Letters*, 93(7):072102, 2008.

[30] H. Huebl *et al. Review of Scientific Instruments*, 80(11):114705, 2009.

[31] C. C. Lo *et al. Physical Review Letters*, 106(20):207601, 2011.

[32] M. Dobers *et al. Physical Review Letters*, 61(14):1650, 1988.

[33] J. van Tol, L. C. Brunel, and R. J. Wylde. *Review of Scientific Instruments*, 76(7):074101, 2005.

[34] G. W. Morley, L. C. Brunel, and J. van Tol. *Review of Scientific Instruments*, 79(6):064703, 2008.

[35] T. Ando, A. B. Fowler, and F. Stern. *Reviews of Modern Physics*, 54(2):437, 1982.

[36] D. Stein, K. v. Klitzing, and G. Weimann. *Physical Review Letters*, 51(2):130, 1983.

[37] D. Stein *et al. Surface Science*, 142:406, 1984.

[38] J. Matsunami, M. Ooya, and T. Okamoto. *Physical Review Letters*, 97(4):066602, 2006.

[39] J. Matsunami, M. Ooya, and T. Okamoto. *Physica E*, 34:248, 2006.

[40] J. Matsunami and T. Okamoto. *Electron Spin Resonance and Related Phenomena in Low-Dimensional Structures, Topics Appl. Physics*, page 129, 2009.

[41] R. E. George *et al. Physical Review Letters*, 105(6):067601, 2010.

[42] A. Morello *et al. Nature*, 467:687, 2010.

[43] J. J. Pla *et al. Nature*, 489:541, 2012.